

Precision synchronization over large Doppler ranges for satellite-based free-space quantum networking

Neal W. Spellmeyer^{*}, Catherine Lee, Marvin Scheinbart, and Scott A. Hamilton
MIT Lincoln Laboratory, 244 Wood St., Lexington, MA USA 02421

ABSTRACT

Precision synchronization is vital for robust long-distance quantum networking over fiber and free-space channels for which high-fidelity entanglement swapping between separate sources via an optical Bell state measurement requires temporal overlap of photonic qubits arriving from either source. This challenge is particularly distinct in satellite-based entanglement distribution in which relative motion, channel effects, and propagation delay must be addressed. This paper describes recent progress on developing and testing a precision synchronization method for free space entanglement distribution in a dual-uplink architecture in which photons from entanglement sources at two ground locations interact in an optical Bell-state measurement implemented on a satellite in a low-earth orbit. The control approach uses independent entanglement sources at each ground location supplemented with a synchronization signal for feedback control from a timing discriminant measured at the spacecraft. The approach is being implemented in a laboratory testbed using 1-GHz repetition rate 1550-nm band entanglement sources generating ~ 10 -MHz source entanglement rates with few-ps photon pulse lengths. The paper describes recent progress towards sub-ps synchronization in large Doppler and Doppler-rate-of-change situations relevant to ground-to-satellite links.

Keywords: Precision Synchronization, Hong-Ou-Mandel, Phase-Locked Loop, Quantum Networking, Quantum Entanglement, Free-Space Communications

1. INTRODUCTION

A central challenge to high-rate entanglement distribution is establishing and maintaining the precision synchronization of interacting photons originating from entanglement sources in different locations [1, 2]. For situations that use spectrally-broad source photons [3] with ~ 1 -ps photon durations, there is a need to synchronize to ~ 0.1 -ps precision. This is especially challenging for long-distance satellite-based entanglement distribution for which photons need to be synchronized over 100-1000-km distances between platforms with ~ 7 -km/s relative motion. Previous work [1, 2] described and implemented a technique for realizing precision synchronization between sources that would be located at two different ground sites and interact at a satellite. In that work, synchronization is achieved by feeding timing information measured at the satellite to the ground locations where the source mode-locked laser (MLL) pulse repetition rate (PRR) is adjusted to close a timing control loop. References [1, 2] described the basic control loop tracking functionality, demonstrated operation in situations of small Doppler rates of change, and discussed extensions of the technique to larger Doppler ranges and rates. This paper describes the implementation and test of those techniques over large Doppler ranges and rates corresponding to situations of practical interest.

The paper is structured as follows. Section 2 gives an overview of the link architecture and the synchronization control methodology. Section 3 describes the laboratory testbed that emulates the dual uplink architecture, and recent upgrades to hardware and control algorithms needed to extend operation to large Doppler ranges and rates. Section 4 describes experimental results achieving < 1 -ps synchronization as the photon arrival time and frequency change over Doppler test profiles representing realistic test cases for links to a satellite in low earth orbit (LEO).

2. LINK ARCHITECTURE AND SYNCHRONIZATION CONTROL

This investigation focuses on an implementation of the dual-uplink architecture [4, 5] which sends entangled photons from sources located at separated ground terminals. One entangled photon from each source is transmitted over a free-space optical link to interact via an optical Bell state measurement (OBSM) at the spacecraft to create shared entanglement between the two ground terminals. This architecture has the advantage of simplifying aspects of the space terminal implementation by keeping resources needed for the entanglement source technology on the ground. The technique is also

^{*} neal@ll.mit.edu

compatible with an uplink/downlink architecture in which entangled photon sources are located at each ground station, and a photon from one source is relayed by the satellite to the other ground station, where it can interact with users in an OBSM.

As described in [1], satellite motion creates a changing time of flight and a change in the apparent PRR and photon wavelength when photons interact in the OBSM. Figure 1 shows Doppler profiles for a representative LEO circular trajectory used as a reference profile for the work described here. For wideband (~ 1 ps) signals, the ~ 30 -part-per-million Doppler shifts are negligible compared to the ~ 400 -GHz optical bandwidth. However, the changing photon arrival times due to changing optical path length are significant compared to the ~ 1 -ps photon duration, indicating that temporal synchronization requires precision temporal control, whereas dedicated wavelength tuning is unnecessary. While the profiles shown here are representative of the Doppler conditions that would be seen in the dual-uplink scenario, the specific relative Doppler profiles would depend on the specific link configurations, including the ground locations relative to the satellite.

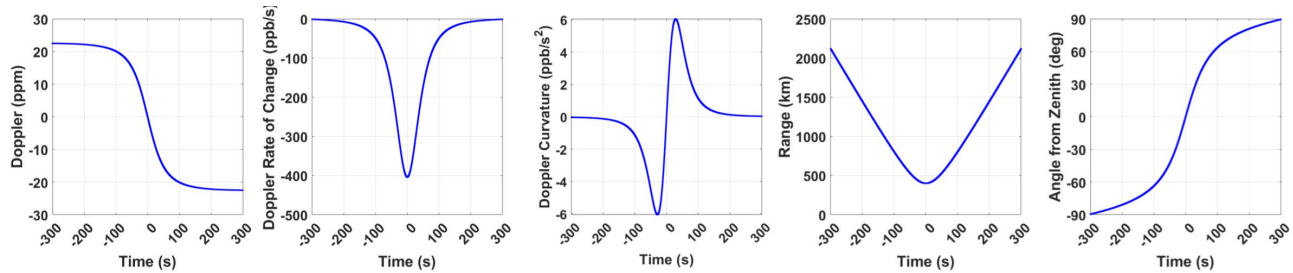


Figure 1. Doppler, Doppler rate of change, Doppler curvature, range, and zenith angle calculated for a circular LEO trajectory. Units are parts per million (ppm) and parts per billion (ppb). All of these quantities affect the synchronization architecture and control loop design.

The essentials of the synchronization control method used here are described in [1]. The technique uses PRR-tunable sources at the ground sites to generate strong timing signals that are measured at the satellite to give good relative timing information about the photons arriving from the two sources. In order to provide the necessary signal flux with sufficient signal-to-noise ratio for high precision control, a weak coherent state photon flux is sent from each ground station in addition to the entangled photons. The relative timing information at the satellite is derived from coincidence counts measured with a Hong-Ou-Mandel (HOM) interferometer. This information is fed to the ground sites, where the MLL PRRs are controlled to establish and maintain alignment of the signals at the satellite. By locking onto the side of the HOM interference dip, the technique is able to achieve sub-ps-level timing at the satellite.

Reference [1] demonstrated the basic viability of the concept, showing performance over a 16-ppb Doppler range and 1.5-ppb/s Doppler rate of change. Reference [2] described a technique for extending the dynamic range of a 16-bit digital-to-analog converter (DAC) used to tune a synthesizer that in turn controls the MLL PRR. The technique monitored the DAC rate of change and then counter-tuned the frequency source to avoid exhausting the DAC range. While the essentials of the technique were demonstrated in [2], additional testbed modifications described in the next section were needed to realize the operation over relevant LEO Doppler ranges as reported in Section 4 below.

3. LABORATORY SYNCHRONIZATION TESTBED

To function over the orbital profiles described above, the synchronization testbed described in [1, 2] was modified in several ways. The testbed (see Figure 2) has dual independent high-rate entanglement sources representing the sources at two ground sites, A and B. These sources operate at near 1-GHz PRR, with a ~ 1 -% slot occupation probability, yielding ~ 10 -MHz source entanglement rate near 1550 nm. A strong classical pump signal is available at either 1550 nm or 775 nm. This work uses superconducting nanowire single photon detectors examining the flux from a 775-nm HOM interferometer. In this testbed, Source A can be considered a transmitter whose PRR is tuned according to a stored Doppler test profile, while Source B can be considered a receiver whose PRR rate is changed by the control loop based on the measured coincidence counts to maintain Source B's temporal alignment to Source A. If the sources are aligned on the side of the HOM dip, then as Source B moves into (out of) alignment, the coincidence counts will decrease (increase), providing a feedback control signal.

A direct digital synthesis (DDS) source (Analog Devices AD9912) that can be updated at fast rates with 48-bit resolution generates the frequency that controls the Source-A MLL PRR. The frequency controlling Source B is created by summing another DDS output with the output of a synthesizer controlled by a 16-bit DAC through an analog frequency modulation port. This allowed a simple way to extend the DAC-based feedback control in [1, 2] to include a smooth and fast frequency ramp consistent with the needs of a type-3 phase-locked loop (PLL) [6] that observes and anticipates the frequency rate of change so that the two sources do not move out of alignment during the infrequent 100-Hz update interval used in this implementation. (A faster update rate would be incompatible with the space-to-ground propagation delay, and lead to loop instabilities.)

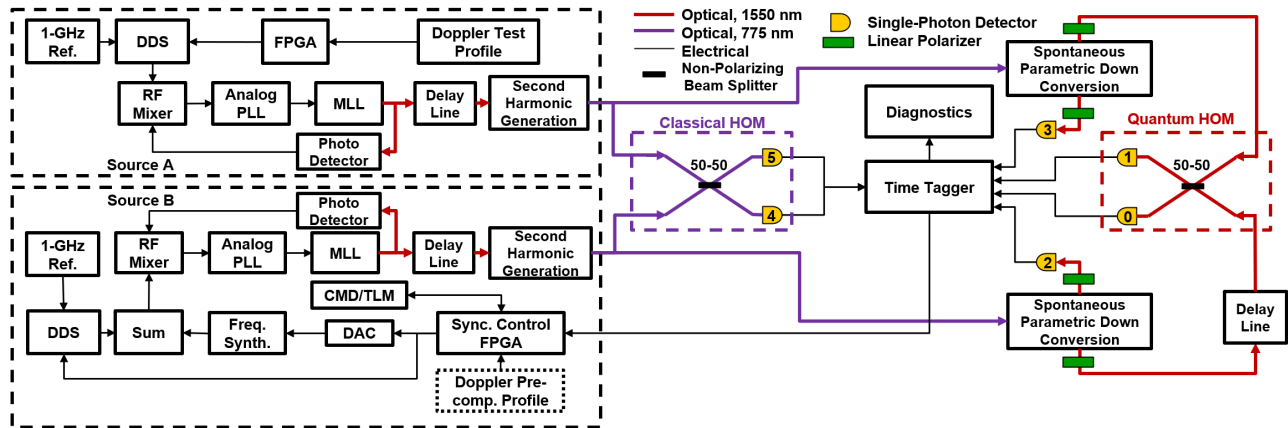


Figure 2. Synchronization testbed block diagram showing key functional elements. Source A and Source B and the spontaneous parametric down conversion sources represent functions at the two ground terminals. A second harmonic generation stage converts the 1550-nm MLL output to 775-nm pulses. The HOM interferometers, single-photon detectors, and time tagger represent functions that would be implemented on the space-side receiver. Real-time time-tagger processing and feedback control loop processing occur in an FPGA. A 16-bit DAC generates a feedback voltage supplied to the frequency modulation port of the Source-B synthesizer. The output of the synthesizer (typically ~300 MHz) is summed with the ~700-MHz DDS output. Fiber-optic motorized delay lines (MDL) provide a fine timing delay capability that can be used for certain measurements, but are not needed for the control loop function itself. PD represents a high-speed photodetector function internal to the MLL that detects the ~1-GHz MLL PRR. Analog PLLs control a tuning port in the MLLs to set their frequency to follow the respective frequency sources with ~1-kHz control loop bandwidth. The Source-A MLL frequency is set by a DDS controlled via a separate FPGA with a pre-programmed Doppler profile representing the orbital motion that would be experienced on the link. A computer provides a command and telemetry (CMD/TLM) interface to the Source-B synchronization control FPGA.

The DAC is adjusted as needed every 0.01 s based on the measured coincidence counts to maintain a particular target coincidence count rate. Between the DAC updates, the DDS source is adjusted at a faster rate (e.g., 1 kHz) based on the observed frequency rate of change in order to create smooth, continuous frequency tuning. As an example of the importance of the update rate, consider the case in which the MLL PRR is updated in single steps at only 100 Hz. For a 100-ppb/s relative Doppler rate of change with a 100-Hz update rate, the frequency of the sources with a 1-GHz PRR would misalign by 1 Hz during the 0.01-s interval, and therefore the relative phase would slip by $\sim(1 \text{ Hz})(0.01 \text{ s})/2=0.005$ cycles, equivalent to 5 ps. This would result in movement off the narrow HOM dip and loss of control. However, if the source is instead updated in 10 smaller steps (each at a 1000-Hz rate) following the observed frequency rate of change, the phase slippage would be the much smaller quantity $10(0.1 \text{ Hz})(0.001 \text{ s})/2=5e-4$ cycles, or 0.5 ps. The testing reported below uses a 4-kHz DDS update rate. The performance limits of this technique are then determined by the quality of knowledge of the Doppler rate of change and curvature.

A single field-programable gate array (FPGA) both processes the counts recorded at the time tagger and implements a digital PLL. In a fielded system, the coincidence processing would be implemented on the receiver, while a low-data-rate, low-latency digital communications channel would send the information to the ground terminals, where the rest of the frequency tuning control loop would be implemented. An inner control loop updates the DAC at a 100-Hz rate, while an outer relaxation loop (see Figure 3) steps the DDS at a frequency rate of change determined by observing the inner DAC control loop plus an input for an optional Doppler pre-compensation profile. The pre-compensation profile would be generated before a session based on ephemeris and expected orbital motion as an estimate of the tuning profile. This would serve to reduce the burden on the control loop, and is expected to be particularly important for initial temporal acquisition.

Note that the results reported below demonstrate control loop tracking, rather than an acquisition capability; the use of a pre-compensation profile has not been necessary for those results.

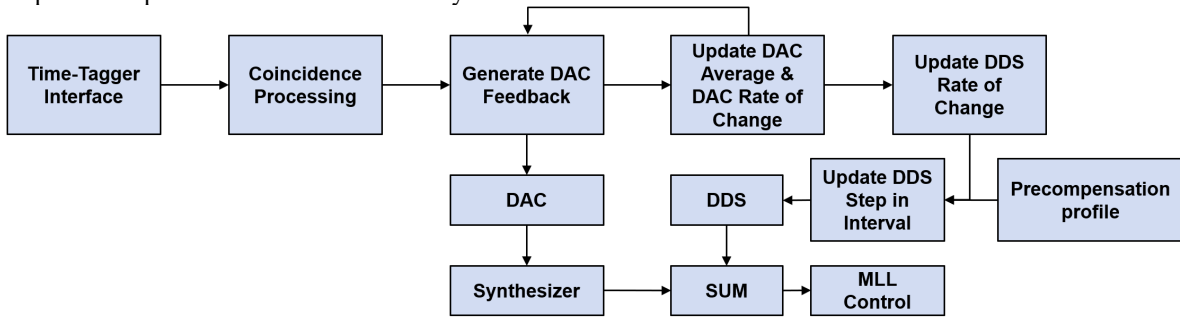


Figure 3. Relaxation algorithm block diagram showing processing flow and associated hardware elements. Photon count time tags pass into an FPGA for coincidence processing, and then into a digital control loop that generates a feedback signal controlling a 16-bit DAC that adjusts the frequency-modulation input to a frequency synthesizer. An analog PLL controls the MLL PRR to match the sum of the synthesizer plus DDS frequencies (close to 1 GHz). An outer control loop within the FPGA observes the DAC rate of change and adjusts the DDS frequency step size so that most of the frequency tuning burden is carried by the DDS. The DAC is updated every 10 ms, while the DDS is updated every 0.25 ms. There is also provision to feed the DDS with a pre-compensation tuning profile.

The space-to-ground propagation delay limits the control bandwidth. For a range of 400 km the round-trip time is 2.6 ms. This work uses a 10-ms control update rate as an approximate representation of the round-trip latency. There is also provision in the FPGA for a delay buffer, which is practical to implement given the relatively small volume of digital coincidence count information. Future testing can explore performance vs. round-trip delay, which is important given the potential for instabilities in the type of control loops investigated here. Other effects, such as fast power fluctuations resulting from atmospheric effects, can also be represented here, although they have not yet been implemented.

4. EXPERIMENTAL RESULTS

To test performance, Source A is tuned according to the Doppler profile shown in Figure 4. This profile is pre-loaded into the FPGA to represent the type of Doppler motion that would be seen at the satellite. This profile has margin against the Doppler range, rate-of-change, and curvature that might be experienced if operating with links to a satellite in LEO (see Figure 1). These profiles use a 4-kHz update rate. For the same reasons as discussed above, the relative timing error of the Source A tuning at a maximum 500-Hz/s frequency rate of change at this update interval vs. an ideal smooth and continuous update would be the negligibly small amount $\sim(1/2)(500 \text{ Hz/s})(0.25 \text{ ms})(0.25 \text{ ms})(1000 \text{ ps/cycle})\sim 0.02 \text{ ps}$. During these tests, temporal acquisition is performed before the start of the Doppler sweep.

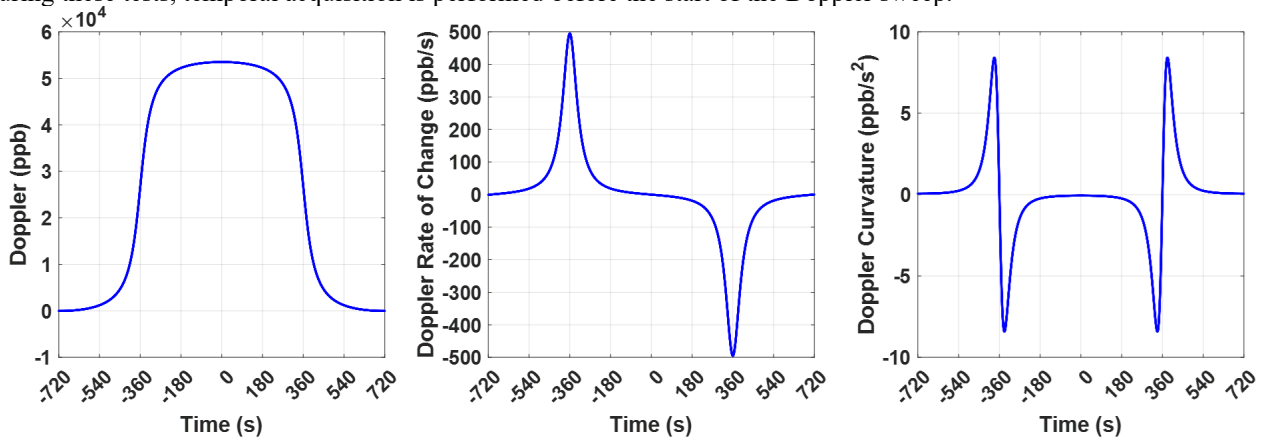


Figure 4. Doppler test profile, showing the Doppler range in ppb (left), Doppler rate-of-change in ppb/s (center), and Doppler curvature in ppb/s² (right). While test profiles are symmetric, sessions on-orbit would entail only one side of the sweeps as a satellite rises on one horizon, passes overhead, and sets on the other horizon. Symmetric profiles are used for convenience and for more thorough testing of the hardware. These profiles use a 0.25-ms DDS update interval.

Similar to the work reported in [1, 2], these tests were conducted with an average signal flux of $\sim 10^7$ counts/s. As discussed in those references, for a random coincidence rate of $\sim 10^5$ counts/s given the $\sim 1\%$ slot occupation probability, there will be ~ 1000 coincidence counts on average in a 10-ms control window. At an operating point on the side of the dip with ~ 750 coincidence counts in the 10-ms control interval, there would be $\sim \sqrt{750} \sim 27$ count fluctuation. For a discriminant slope of ~ 130 counts per 10-ms interval per ps of timing delay (130 counts/10 ms/1 ps), this implies an expected timing control uncertainty of $\sim 27/130 = 0.2$ ps.

Figure 5 shows measured control loop telemetry from a test in which Source A was swept over the profile from Figure 4. The results show stable precision locking of Source B to Source A on the side of the HOM dip. The ~ 30 -count peak-to-peak variation in average coincidence count during the test implies $\sim 30/130 = 0.25$ -ps relative timing variation. As expected, the peak deviation occurs when the frequency sweep rate is largest. These small deviations are expected given the type-3 control loop that must observe and anticipate the large frequency sweep rate given the ~ 100 -Hz control loop update rate which is driven by the space-to-ground latency. During the sweep, the 16-bit DAC moves as necessary to keep the sources aligned on the side of the HOM dip. As the frequency rate of change increases and the DAC follows, the outer control loop observes the motion of the DAC and commands the DDS to move at a similar rate. This outer control loop detects and absorbs most of the frequency change that occurs, enabling good performance over the large Doppler range. Note also that these results confirm the MLLs can sweep in a fast and smooth manner over the large test range.

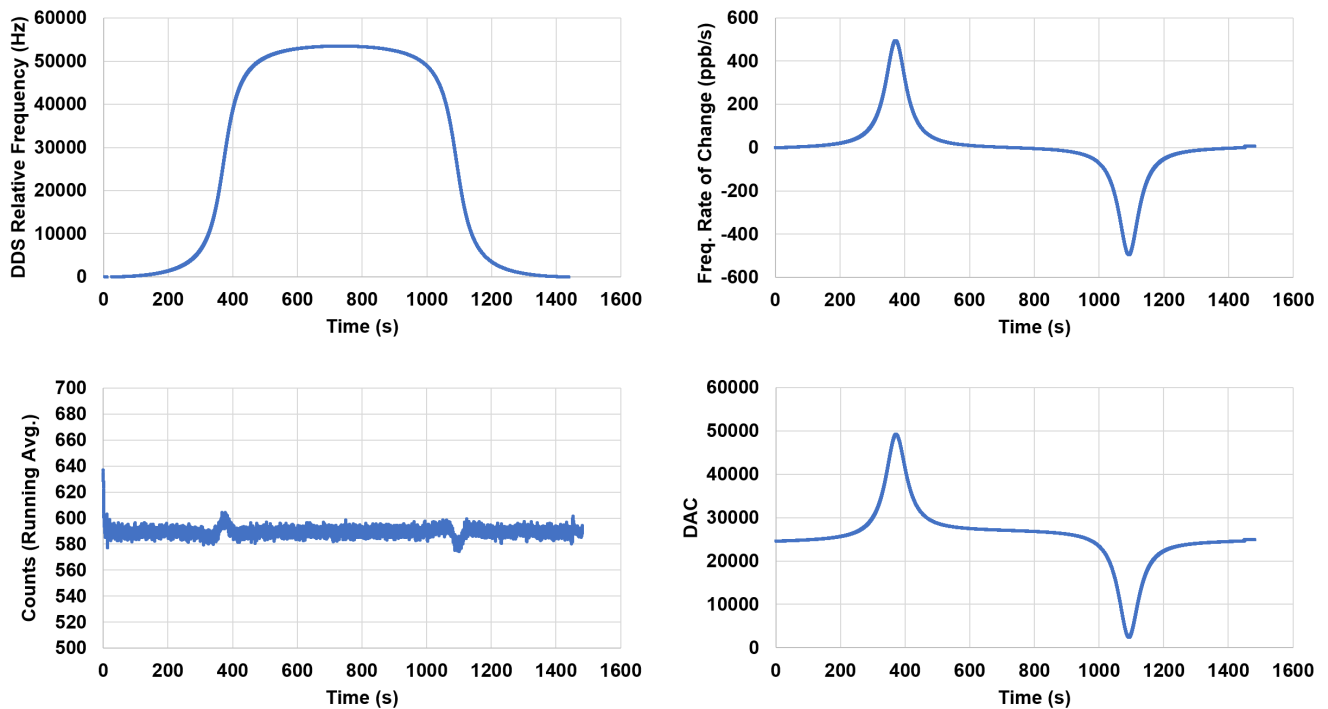


Figure 5. Control loop telemetry collected during a sweep over the test profile shown in Figure 4. Upper left: Source-B DDS relative frequency. Upper right: frequency rate of change. Lower left: a running average of the HOM coincidence counts collected during the session, showing stable locking on the side of the HOM dip. The small features occurring during the maximum frequency rate of change arise from the type-3 control loop interacting with the large rate of change. Lower right: the 16-bit DAC set point recorded during the sweep. Note that for a calibration of ~ 4 Hz/1000 DAC steps, the DAC moves by < 400 Hz during the sweep, with the much larger range being absorbed by the DDS.

5. SUMMARY

This work has described the extension of a method for precision synchronization suitable for long-distance quantum networking, and demonstrated its performance in a laboratory testbed. The technique uses MLL PRR control as the primary mechanism to correct for changes in range and rate due to orbital motion. It uses a sensitive HOM-based timing discriminant which minimizes the photon flux needed for synchronization. The work described here has extended the hardware and control loop FPGA code to be able to operate over Doppler ranges and rates that would be encountered in operation with a satellite in LEO. Work is underway to extend the techniques to support efficient, automated temporal acquisition.

DISTRIBUTION STATEMENT A. Approved for public release. Distribution is unlimited.

This material is based upon work supported by the National Aeronautics and Space Administration under Air Force Contract No. FA8702-15-D-0001. Any opinions, findings, conclusions or recommendations expressed in this material are those of the author(s) and do not necessarily reflect the views of the National Aeronautics and Space Administration.

©2024 Massachusetts Institute of Technology

Delivered to the U.S. Government with Unlimited Rights, as defined in DFARS Part 252.227-7013 or 7014 (Feb 2014). Notwithstanding any copyright notice, U.S. Government rights in this work are defined by DFARS 252.227-7013 or DFARS 252.227-7014 as detailed above. Use of this work other than as specifically authorized by the U.S. Government may violate any copyrights that exist in this work.

REFERENCES

- [1] N. Spellmeyer et al., "Precision Synchronization for Free-space Quantum Networking," *SPIE Quantum West*, paper 124460G, (2023).
- [2] N. Spellmeyer et al., "Precision Synchronization for Long-distance Free-space Quantum Networking," *Optica Quantum 2.0 Conference*, paper QW3A.5 (2023).
- [3] C. Lee et al., "Bright, Waveguide-based Entanglement Sources for High-rate Quantum Networking," *Optica Quantum 2.0 Conference*, paper QTh4A.7 (2022).
- [4] M. Aspelmeyer et al., "Long-Distance Quantum Communication With Entangled Photons Using Satellites," *IEEE J. Sel. Top. Quantum Electronics*, vol. 9, no. 6, pp. 1541-1551, Nov/Dec. 2003.
- [5] N. Hardy, P. B. Dixon, and S. A. Hamilton, "Teleportation Fidelity Improvement with Quantum Memory," *Optica Quantum 2.0 Conference*, paper QM4B.4 (2022).
- [6] F.M. Gardner, *Phaselock Techniques*, John Wiley & Sons, Third Edition, 2005.